Reactant states model: Predicted $k(E,J)$ for $NO_2(^2A_1) \rightarrow O(^3P) + NO(^2\Pi)$, based on spectroscopic data

Beatriz M. Toselli and John R. Barker[a)]
Department of Atmospheric, Oceanic, and Space Sciences, Space Physics Research Laboratory, The University of Michigan, Ann Arbor, Michigan 48109-2143

(Received 24 August 1988; accepted 28 April 1989)

High-order spectroscopic data for the reactant are used *exclusively* to determine both the sum of open reactive channels and the density of states, which are used in a statistical theory to predict dissociation rate constants. Practical methods are introduced for calculating sums of reactive channels and densities of states, when *couplings among all degrees of freedom are included*. An empirical method is described for reconciling spectroscopic parameters with known dissociation energies (also determined spectroscopically). The predicted $k(E,J)$'s and thermal $k_\infty(T)$ for NO_2 dissociation are in good agreement with experimental data, especially when the effects of electronically excited states are included. The predicted low pressure thermal rate constants are generally in fair agreement with experiment, although a slightly different temperature dependence is calculated; this discrepancy is probably due to the absence of unknown higher order spectroscopic terms and to the crude corrections made for excited electronic states. When high order spectroscopic (or theoretical) data are available and when the effects due to excited electronic states are considered, this theory is useful for predicting, fitting, and interpreting unimolecular rate data.

1. INTRODUCTION

Unimolecular reaction rate theory has developed steadily[1-3] ever since Lindemann proposed[4] that there is a delay between the time a reactant is energized and the time it reacts. Due to the complexities of dynamical systems with many degrees of freedom, statistical approaches have proved to be the most successful. The venerable RRKM theory[5] is a statistical theory that has been tested many times and has been found to be very useful for treating unimolecular reaction rate constants.

The central premise of RRKM theory is that energy is rapidly distributed among all of the active degrees of freedom in an excited reactant. In addition, it is assumed that microcanonical Transition State Theory can be used to describe the act of decomposition. Recent experiments support the first premise under most conditions, although exceptions have been identified in a few cases.[6-8] The second assumption is generally supported by the results of classical trajectory calculations, but there are some exceptions.[9-12]

A weakness of conventional applications of transition state theory is that the properties of the transition state are rarely available, except when the potential energy surface (PES) is calculated. Semiempirical adaptations of RRKM theory[13] and empirical correlations of experimental data have proven to be very useful in overcoming this handicap,[14] but the purely predictive capabilities[15] of the theory remain relatively modest. In many applications, spectroscopic data are used as a starting point for estimating transition state parameters, but no consistent procedure has been developed for this purpose and normally only the lowest order spectroscopic parameters are used.

In RRKM theory, the transition state essentially is a device for calculating the number of reactive channels (also called exit states, unbound states, etc.) that connect reactant states with product states. Phase space theory utilizes product state counting to determine the number of reactive channels, subject to conservation of total energy, parity, and angular momentum.[16,17] In the statistical adiabatic channel model (SACM),[18] Quack and Troe used a combination of product state counting and empirical potential energy functions to estimate the number of reactive channels; when available, exact potential energy functions can be employed in the theory.[19] Other unimolecular reaction theories (e.g., Slater Theory[20] and that developed by Pritchard[21]) have also been developed, but will not be described here.

Most statistical theories of unimolecular reactions (which involve formation of a strongly coupled complex[22] at microcanonical equilibrium) produce an expression for the specific reaction rate constant that can be reduced to the following form for dissociation reactions.[23,24]

$$k(E) = \frac{1}{h}\frac{G(E)}{N(E)}, \tag{1}$$

where $G(E)$ is the sum of states that correlate with product states (sum of open channels, unbound states, etc.), h is Planck's constant, and $N(E)$ is the total density of states of the reactant. In RRKM theory, $G(E)$ is the sum of states of the transition state; in phase space theory, $G(E)$ is the sum of open channels that correlate adiabatically with the product states. When the PES is known, all of these theories can be applied in their appropriate limits of validity. Unfortunately, the PES is rarely known for applications to real systems and various empirical approximations must be introduced.

Equation (1) has been derived in several ways.[2,3,5,18,24] Miller[25,26] showed that the canonical rate constant can be written

$$k(T) = \frac{1}{hQ_R}\int_0^\infty dE\, F(E)\exp(-E/kT), \tag{2}$$

where Q_R is the reactant partition function and $F(E)$ is pro-

[a)] Also Department of Chemistry.

 0021-9606/89/162239-15$02.10

portional to the classical flux of representative mass points through a dividing surface.[27] The canonical rate constant $k(T)$ is the thermal average of the microcanonical rate constant $k(E)$:

$$k(T) = \frac{1}{Q_R} \int_0^\infty dE\, k(E) N(E) \exp(-E/kT) , \quad (3)$$

where $N(E)$ is the density of states of the reactant, given by

$$N(E) = h^{-s} \int\int d\mathbf{p}\, d\mathbf{q}\, \delta[E - H(\mathbf{p},\mathbf{q})] . \quad (4)$$

Here, the coordinates $\mathbf{q} = \{q_i\}$, $i = 1, \ldots$ and conjugate momenta $\mathbf{p}$ are the variables in the classical Hamiltonian $H(\mathbf{p},\mathbf{q})$; the Dirac delta function ensures the integration in Eq. (4) is carried out for $H(\mathbf{p},\mathbf{q}) = E$. The ranges of integration in Eq. (4) depend on the location of the dividing surface between reactants and products, and $N(E)$ includes all states, whether bound, or unbound. Note that $F(E)$ can be identified with the sum of unbound states $G(E)$.

In this paper, high order spectroscopic data are used directly to calculate both $G(E)$ and $N(E)$ in Eq. (1). Our motivation is to minimize the empiricisms and assumptions needed in real applications, and still circumvent the need for determining the PES, which is a difficult and laborious task. The resulting model differs significantly from the others mentioned above, although there are naturally strong similarities. The present approach does not assume separability of the internal degrees of freedom; intermode couplings are explicitly included, based on the spectroscopic data for the species involved. No transition state need be defined. Instead, the present approach uses high-order spectroscopic data to identify the unbound states and to calculate the density of states.

The spectroscopic constants used in this formulation include vibrational frequencies, diagonal and off-diagonal anharmonicities of all orders, rotational constants, centrifugal stretching coefficients, etc. Generally speaking, the complete set of these spectroscopic data is never available, but important and useful subsets of data are available for many species and theoretical calculations[28] may provide some of the missing spectroscopic data. To compensate for the absence of crucial spectroscopic data and to reconcile disparate spectroscopic data, some empiricism must be introduced, but we have endeavored (with some success) to minimize it.

Although NO_2 is one of the kinetically best-characterized reactants, its spectroscopic puzzles are notorious. The ground state spectroscopic properties are of the most immediate interest in the present work, but rovibrational states above $\sim 8500\,cm^{-1}$ have not been assigned.[29,30] Thus, a long extrapolation of spectroscopic properties to the dissociation limit[31] ($\sim 25\,132\ cm^{-1}$) is necessary. This extrapolation may be even more complicated due to the poorly understood mixing[32] of the three excited electronic states with the ground state.[33] The influence of the excited electronic states on the kinetics is also not well understood, and it may well be important.[34]

It is shown in this paper that despite the limitations imposed by the long extrapolations of spectroscopic data and the uncertainties introduced by electronically excited states, the predicted $k(E)$ values are in good agreement with experiment; thermal rate constants are in fair agreement, but they are much more sensitive to small errors in threshold energy and are therefore less reliable. This theoretical method shows considerable promise for predicting $k(E,J)$ for molecules with well-known spectroscopic properties and it may provide an important testing ground for statistical unimolecular rate theories.

II. THEORY

A. Approximate reduction to one dimension

In conventional RRKM theory, a convenient approximation is to assume that the PES is separable in the vicinity of the transition state. This approximation permits the problem to be reduced to a single dimension and the one-dimensional problem is then solved.[35] A related strategy is employed here, but separability is not assumed.

Reactants that can decompose are intrinsically anharmonic and therefore the harmonic oscillator model, which can never dissociate, is completely unsuitable. The simplest vibrational model for molecules that can decompose has vibrational states with quadratic dependence on vibrational quantum numbers (neglecting Fermi resonances, Coriolis coupling, and other perturbations). A better description includes even higher-order anharmonicities, as described by the following spectroscopic term expression, for example:

$$E = \sum_{i=1}^{n} v_i \omega_i^0 + \sum_{i=1}^{n}\sum_{j=1}^{n} X_{ij} v_i v_j + \sum_{i=1}^{n}\sum_{j=i}^{n}\sum_{k=i}^{n} y_{ijk} v_i v_j v_k . \quad (5)$$

Here, v_i is the quantum number for the ith vibrational mode, ω_i^0 is its frequency, and X_{ij} and y_{ijk} are the quadratic and cubic anharmonicities, respectively. Note that the frequencies and anharmonicites are also modified by couplings with rotations and other conserved degrees of freedom (DOF), which, for simplicity, are not written explicitly.

Equation (5), which is a power law expansion, cannot be expected to describe with great accuracy the vibrational states of a molecule at very high energies. Indeed, if the states are strongly coupled, no simple power law expansion may be a good description and the states may not even be assignable.[36] Under these circumstances, we will assume that the power law expansion (or some other expansion, such as in a local mode basis) describes the *average* behavior suitable for state counting. One strategy for improving these extrapolations has been based on theoretical consideration of the expected long range potentials for diatomics,[37] perhaps a similar approach could be used for polyatomic molecules.

For total energy E, quantum numbers can be assigned to all modes, except the last ($i = n$), and the equation can be rearranged to give the residual energy U as a function of the quantum number v_n associated with the last coordinate[38]:

$$U(v_n) = E - \sum_{i=1}^{n-1} v_i\omega_i^0 - \sum_{i=1}^{n}\sum_{j=1}^{n-1} X_{ij}v_jv_i + \sum_{i=1}^{n}\sum_{j>i}^{n}\sum_{k>j}^{n-1} y_{ijk}v_iv_jv_k = \left\{\omega_n^0 + \sum_{i=1}^{n-1} X_{in}v_i + \sum_{i=1}^{n-1}\sum_{j=i}^{n-1} y_{ijk}v_iv_j\right\}v_n + \left\{X_{nn} + \sum_{i=1}^{n-1} y_{ijk}v_i\right\} n^2 + y_{nnn}v_n^3 . \quad (6)$$

Equation (6) has the form $U(v_n) = \omega v_n + Xv_n^2 + yv_n^3$; if the cubic anharmonicity equals zero, $U(v_n)$ has the functional form appropriate for several one-dimensional oscillators, including the Morse oscillator and the oscillator with potential energy $V(q) = -U_0/(\cosh^2 aq)$[39] and this suggests that one of these potentials is the approximate *effective one-dimensional potential* for the last degree of freedom in the field of all of the other degrees of freedom.

Generally, *the form of the effective one-dimensional potential is not known and is not necessary for present purposes*, but Fig. 1 shows the relationship between the actual effective potential and a Morse function (for example) deduced from spectroscopic data. In principle, the correspondence can be very close up to the highest bound level, but beyond that point the actual potential may diverge. Actual spectroscopic term expressions are usually more complicated than Eq. (5), since other degrees of freedom must be included. For example, the expression for a prolate symmetric top is given by Eq. (7), which is based on the Watson Hamiltonian.[40]

$$E(\mathbf{v},J,K) = \sum_{i=1}^{n}\omega_i^0 v_i + \sum_{i=1}^{n}\sum_{j=i}^{n} X_{ij}v_iv_j + \sum_{i}^{n}\sum_{j=i}^{n}\sum_{k=j}^{n} y_{ijk}v_iv_jv_k - \sum_{i}^{n} v_i\alpha_i^{0A}K^2 + \sum_{i}^{n} v_i\beta_i^0K^4 - \Delta_J J^2(J+1)^2 - \Delta_{JK}J(J+1)K^2 - \Delta_K K^4 + H_J J^3(J+1)^3 + H_{JK}J^2(J+1)^2K^2 + H_{KJ}J(J+1)K^4 + H_K K^6 - L_K K^8 - \sum_{i}^{n} v_i\alpha_i^{0B}[J(J+1) - K^2] + \sum_{i}^{n}\sum_{j>i}^{n}\gamma_{ij}^0 A v_iv_jK^2 + B_0J(J+1) + (A_0 - B_0)K^2 . \quad (7)$$

When rotational degrees of freedom are included, the one-dimensional effective potential in Fig. 1 may have a centrifugal maximum; the dissociation energy of the one-dimensional potential (e.g., Morse potential) then approximates the maximum of the effective potential, as illustrated. Note that because the present theory does not make direct use of potential energy functions and transition state dividing surfaces, variational transition state theory[41] is not applicable.

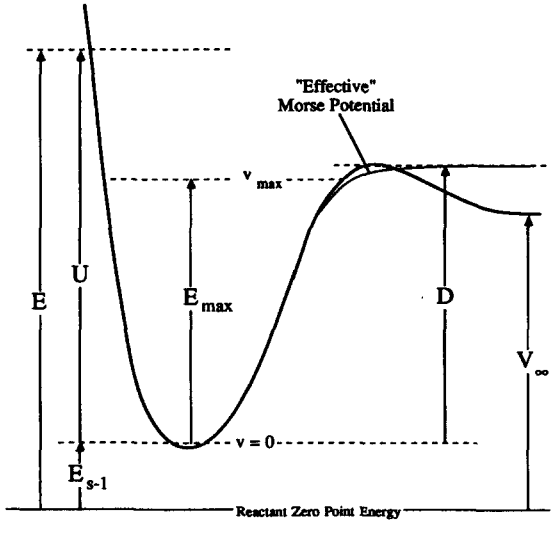

FIG. 1. Definitions of energies used in the present work. The potential energy curve is for the critical coordinate. Note that the actual effective potential (derived from spectroscopic terms) can be fitted with a Morse curve up to the energy E_{max} corresponding to the top-most bound state.

For a molecule with s nondegenerate rotational and vibrational degrees of freedom, the ith bound state can be described by a vector of quantum numbers $\mathbf{v}_i = \{\mathbf{v}_{s-1}, v_s\}_i$, where $\mathbf{v}_{s-1}$ is the vector of quantum numbers for the $s-1$ DOF and v_s is the quantum number for the last DOF. These quantum numbers include all of the vibrational quantum numbers, as well as the rotational quantum numbers J and K. If the last DOF is treated classically, while all of the others are assigned quantum numbers, the ith state can be designated $\{\mathbf{v}_{s-1}\}_i$. Since total energy E has been specified, the designation of $U(v_s)$ [see Eq. (6)] is unnecessary. For each $\{\mathbf{v}_{s-1}\}_i$, the effective one-dimensional potential for the last coordinate q_s will depend on all of the other quantum numbers (due to coupling), producing bound state energies described by an equation analogous to Eq. (6). If the last DOF is a vibration, its effective frequency and anharmonicities thus depend *parametrically* on $\mathbf{v}_{s-1}$: $\omega(\mathbf{v}_{s-1})$, $X(\mathbf{v}_{s-1})$, and $y(\mathbf{v}_{s-1})$; if it is a rotation, the rotational constants depend parametrically on $\mathbf{v}_{s-1}$.

For the purpose of state counting, we will assume that the last DOF can be described with an effective one-dimensional potential energy function that depends parametrically on $\mathbf{v}_{s-1}$. Knowledge of the functional form of the potential energy $V_s(\mathbf{v}_{s-1}, q_s)$ is not necessary for present purposes, but the dissociation energy of the potential is needed in order to distinguish between bound and unbound states. According to the usual method for potential functions that support a finite number of bound states (neglecting tunneling through a barrier), the dissociation energy $D(\mathbf{v}_{s-1})$ is the energy where a true continuum exists and the energy spacing between adjacent states vanishes. For one dimension, this condition can be written

$$\left(\frac{dU}{dv_s}\right)_{U=D} = 0. \tag{8}$$

Here, $U(v_s)$ is an expression analogous to Eq. (6). Each "state" $\{\mathbf{v}_{s-1}, v_s\}_i$ with total energy E can be identified as bound, or unbound, depending on whether $U(v_s)$ is less than $D(\mathbf{v}_{s-1})$, or (equivalently) $v_s \leqslant v_{s,\max}$ (the highest bound level). A state that is *unconditionally* bound is one which has all positive partial derivatives of U with respect to the nonconserved quantum numbers (neglecting tunneling):

$$\left(\frac{\partial U}{\partial v_i}\right)_{\mathbf{v}_{j\neq i}} > 0 \quad \text{for } i = 1, 2, ..., s. \tag{9}$$

This is a generalization of Eq. (8) to many quantum numbers. States that do not satisfy the condition (9) are unbound in one, or more DOF. [Note that the condition applies to rotations, as well as vibrations, in prolate symmetric top molecules, because the energy increases as the K quantum number is increased; for oblate tops, the test is reversed, since the energy decreases as K increases.]

We assume that unbound states can be labeled according to the vector $\mathbf{v}_{s-1}$. This identification is rigorously correct only as long as the $s-1$ DOF are not coupled to the continuum and are therefore adiabatic. In this case, the energy of the state is the sum of the energy in the last DOF and that in the adiabatic DOFs; the energy in the DOFs is described by an equation analogous to Eq. (5). For the purpose of state counting, we assume this description to be valid, even when the DOFs are coupled to the continuum. This assumption can be tested in future work by determining whether the average positions of scattering resonances are described by equations analogous to Eq. (5). In the present work, the test of this assumption is the performance of the model in predicting rate constants.

B. Sum of reactive states

In order to count the total number of reactive states, we can select a DOF and designate it the "critical" DOF (coordinate), and then determine the sum of states which are unbound with respect to this critical coordinate. Since more than one DOF may have unbound states, this process must be repeated for all of the DOF to obtain the total number of states which are unbound. Note that there may be states that are simultaneously unbound in more than one coordinate, but, at moderate energies, the number of these states is expected to be much smaller than the number that are unbound in a single coordinate, and they will be neglected in the present work.

First, the DOF are ordered so that the critical DOF is last, and each quantum state at total energy E is designated as above: $\{\mathbf{v}_{s-1}\}_i$. The sum of reactive states corresponding to a single critical DOF is the number of $\{\mathbf{v}_{s-1}\}_i$ vectors that leave enough energy in the critical coordinate so that it is unbound. In other words, for each $\{\mathbf{v}_{s-1}\}_i$, U_i is tested according to Eq. (9); if it fails the test, the state is assumed to be reactive and to contribute to $G_q(E)$, the sum of reactive states when the qth DOF is unbound. When the off-diagonal anharmonicities and other coupling coefficients are nonzero, several different modes can react and the total sum of reactive states is $G(E) = \Sigma_q G_q(E)$.

For small reactants, $G(E)$ can be determined by brute force evaluation of Eq. (6) for every combination of quantum numbers for the nonconserved noncritical DOF. For larger reactants, high efficiency Monte Carlo methods are preferred, and one such method is described in a later section.

C. Density of states

For bound states we use the following relationship, where the quantum number v_s is treated as a continuous variable:

$$\rho(U) = \left[\left(\frac{\partial U}{\partial v_s}\right)_{\mathbf{v}_{s-1}}\right]^{-1}, \quad U < E_{\max}. \tag{10}$$

For a Morse oscillator, for example, this expression is just

$$\rho(U) = \frac{1}{\omega[1 - U/D]^{1/2}}. \tag{11}$$

For any potential, Eq. (10) is applicable for energies up to that of the topmost bound state ($E_{\max}$ at $v_{\max}$).

For the narrow range of energies below D, but above $E_{\max}$, Eqs. (10) and (11) cannot be used, because they are singular when $U = D$ and $\rho(U)$ would be grossly overestimated. To avoid this problem, we make the simple assumption that $\rho(U) = \rho(E_{\max})$ for $D > U > E_{\max}$. An alternative approach might be to apply the "tau method": for motion in one dimension, $dpdq = dEdt$; integration of Eq. (4) over energy and period $\tau_v(E)$ gives

$$\rho(U) = h^{-1}\tau_v(U), \tag{12}$$

where $\tau_v(U)$ is the time period for "vibration." For bound states, this is the period for vibration between inner and outer classical turning points, while for energies above the dissociation limit, is twice the time necessary for the motion from the inner turning point to the dividing surface separating reactants and products.[42] The potential might be assumed to be a Morse curve and a reasonable choice of the dividing surface is the outer classical turning point of the topmost bound level.[43,44]

Considering the effective one-dimensional model described above, each vector $\{\mathbf{v}_{s-1}\}_i$ has a corresponding density of states $\{\rho(U)\}_i$, which is given by Eq. (10). If the total number of $\{\mathbf{v}_{s-1}\}_i$ vectors (bound states) at energy E is $W_b(E)$, then the total density of bound states is the sum of the individual contributions:

$$N_b(E) = \sum_{i=1}^{W_b(E)} \{\rho(U)\}_i. \tag{13}$$

This summation can be evaluated by Monte Carlo methods, as described in a later section.

For unbound states, Eq. (10) cannot be applied, because it is inappropriate for energies greater than the dissociation limit, and so we resort to another method. We first calculate the sum of unbound states $G(E)$ as described above and then differentiate it[2,3] to determine the density of unbound states:

$$N_u(E) = \frac{dG(E)}{dE}. \tag{14}$$

The total density of states is then the sum of the two terms:

$$N(E) = N_b(E) + N_u(E). \quad (15)$$

Our calculations[45] show that for molecules larger than triatomics at moderate energies, $N_u(E)$ can be neglected to an excellent approximation [this finding partially supports the implicit assumption made in every other calculation of which we are aware, that $N_u(E)$ makes a negligible contribution to $N(E)$]. However, *in the limit of very high energies, there are no bound states and every state is unbound, regardless of the size of the molecule.* Thus $N_u(E)$ must be included at high energies, even for large molecules.

The Monte Carlo methods used in the present work to obtain $N_b(E)$ and $G(E)$ are described below.

D. Symmetry and reaction path degeneracy

Statistical factors originate from two sources in the present work: the usual symmetry factors and unbound state degeneracies (bound states are assumed to be nondegenerate, aside from symmetry factors).

Unbound state degeneracies can be determined as follows. Consider the curved reaction path q corresponding to the dissociation of NO_2 into NO + O. The potential profile along that path is an even function that roughly resembles the $1/\cosh^2 aq$ one-dimensional potential, which has the same expression for the energy levels as the Morse oscillator. Separation of the reaction products can occur at both $q = +\infty$ and $q = -\infty$ (to produce O + NO and ON + O, which are indistinguishable), leading to a degeneracy of two[39] for states above the dissociation energy. For all symmetric potentials and equivalent products (isotopic substitution can produce nonequivalent products), the translational wave function degenerate pairs can be identified as even, or odd functions, and this symmetry property can be used to categorize the wave functions.[39] Odd potential functions, such as the Morse oscillator, can only decompose for positive values of q and therefore the degeneracy of unbound states is unity. The Morse potential is qualitatively appropriate for symmetric stretch modes and other modes where the potential can only decompose for one direction of motion.

The degeneracy g_u of the unbound critical oscillator states must be used in the evaluation of both $N_u(E)$ and $G(E)$. For one-dimensional motion along the critical coordinate, g_u is determined according to whether dissociation is possible in only one direction, or in both directions. However, the potential surface is not one dimensional and the actual motion at any point can be described in terms of a linear combination of coordinates. For NO_2, the dissociation energy of the symmetric stretching mode is lowered when energy resides in the asymmetric stretch mode (see below) and the motion is some combination of the symmetric stretch q_1 and the asymmetric stretch q_3 coordinates. Since the molecule can dissociate both toward $(q_1, q_3) = (+\infty, +\infty)$ and $(q_1, q_3) = (+\infty, -\infty)$, the translational wave function is doubly degenerate and $g_u = 2$ whenever the quantum number $v_3 > 0$, but $g_u = 1$ when $v_3 = 0$ (in the calculations reported below, the great majority of unbound states had $v_3 > 0$).

As discussed by Pollak and Pechukas[46] and by Coulson,[47] symmetry factors should be used in the partition functions in transition state theory, rather than other prescriptions for "reaction path degeneracy." Similarly, $G(E)$ and $N(E)$ must include all appropriate symmetry factors σ_s, if the density of states is high enough for their use. For a symmetrical molecule like $NO_2(C_{2v})$, each state with specified J quantum number must have a particular symmetry with respect to interchange of the two oxygen nuclei.[18] Thus, regardless of the value of J, only half of the rovibrational states occur in NO_2, on the average (if the density of states is not sufficiently large, the average cannot be applied). *The same principle applies to unbound, as well as to bound states.*

The unbound state symmetry is determined according to the same rules as for bound states, but the symmetry of the unbound "vibration" is determined according to whether the translational wave function in the critical coordinate is even or odd. For the unbound asymmetric stretching mode (symmetric potential energy function) in a symmetric triatomic, half the translational wave functions are even and half are odd. If the states are closely spaced, the total *mechanical density* of states is divided by $\sigma_s = 2$, the rotational symmetry number. Similarly, the *mechanical sum* of unbound states is also divided by σ_s. Since both numerator and denominator of the rate constant expression are divided by the same factor, the symmetry factors cancel, unless the states are so widely spaced that the average symmetry factor cannot be used and individual state symmetries must be evaluated.

The final expressions for the sum of unbound states and the total density of states, including both symmetry factors and the degeneracy of unbound states, are given by

$$G(E,J) = \sigma_s^{-1} \sum_{i=1}^{W_u(E,J)} \{g_u\}_i \quad (16a)$$

$$N(E,J) = \sigma_s^{-1} \sum_{i=1}^{W_b(E,J)} \{\rho(U)\}_i + \frac{d}{dE} G(E,J), \quad (16b)$$

where $W_b(E,J)$ and $W_u(E,J)$ are the "mechanical" sums of bound and unbound states (neglecting statistical factors), respectively, and where the symmetry factors are written explicitly, although they cancel in Eq. (1). A Monte Carlo method for evaluating these functions is presented below.

It is interesting to compare the magnitudes expected for the rate constants for dissociation of NO_2 molecules that may have isotopically labeled oxygen atoms. If one oxygen is labeled, but the spectroscopic constants are unchanged from the unlabeled molecule, the dissociation energies to produce O* + NO and O*N + O are identical, making $\sigma_s = 1$, but g_u may still equal 2, if v_3 is excited. The symmetry number σ_s cancels in Eq. (1) and g_u depends not on symmetry, but on whether dissociation can take place in two directions[39] and thus is not affected by the labels. The result is that the rate constants for dissociation of ONO and O*NO are identical, if their spectroscopic constants are the same, as is expected. The branching ratio to form the two sets of labeled products is not predicted explicitly by the present theory, and additional assumptions will be necessary for its evaluation.

III. COMPARISONS WITH OTHER THEORIES

In the present theory, $G(E)$ is calculated from the spectroscopic constants and corresponds only to the unbound

states of the reactant. The criterion for identifying an unbound state is based on whether the energy in the critical coordinate exceeds the effective dissociation energy in that coordinate. Due to the coupling among the coordinates, it is also necessary to test whether the energy in any other coordinate exceeds its dissociation energy, after all of the quantum numbers have been assigned. That is the basis for the tests in Eq. (9).

In the usual applications of RRKM theory,[2,3,5] $G(E)$ is calculated based on a transition state described by empirical parameters that fit experimental kinetics data, or (rarely) from calcuated PESs. Only recently, intermode couplings have been included in the evaluation of $G(E)$ from potential surfaces,[48,49] but, in most applications, the DOF are assumed to be separable. In most practical applications, the reactant and the transition state are treated as distinct chemical species, as is suggested by the form of transition state theory, where the transition state has one fewer DOF than the reactant. By contrast, in the present approach, there is only one chemical species, but only certain of its states are identified as reactive states. In our language, the transition state can be regarded as a device that helps in the determination of the sum of unbound states and its (usually) empirical parameters compensate for neglect of the intermode couplings, which are specifically included in the present theory. The correspondence between the present approach and the transition state species is clear, if it is noted that a transition state species can be defined (but not uniquely!) that has a *total* sum of states equal to the sum of *unbound* states of the reactant in the present approach.

In the usual applications of RRKM theory, separable degrees of freedom are assumed and therefore states of the transition state are independent of the exact distribution of energy among the noncritical DOF. By contrast, the unbound states in the present theory depend on every unique combination of the noncritical DOF quantum numbers, due to the specific inclusion of intermode couplings. An important advance beyond conventional RRKM theory has been made by Wardlaw and Marcus,[49] who employ Monte Carlo integration of the classical phase space integral to obtain the sum of states for the "transitional" modes, which are usually strongly coupled.

The Quack and Troe SACM,[18] in its simplest version, specifically considers a small number of intermode couplings by invoking semiempirical coupling factors. In this theory, $G(E)$ is the sum of open adiabatic channels which are assumed to correlate with the product states. The adiabatic channels are constructed from assumed potential energy curves and associated centrifugal barriers, thermochemistry, semiempirical corrections for coupling between the reaction coordinate and other degrees of freedom, and rules for correlating reactant and product states. The present theory resembles the SACM in that the reactant unbound states can be identified approximately with the open adiabatic channels of the SACM, but the two theories differ in the methods used for identifying the unbound states and calculating molecular state densities.

In all applications of which we are aware in which the PES is not known, RRKM theory and the SACM have included only the density of bound states for anharmonic oscillators in the denominator of Eq. (1) (the harmonic oscillator approximation can be used to estimate the total density of states, but this approximation is very poor for energies near and above the reaction threshold). The present theory includes the densities of both bound and unbound states in practical calculations. For triatomic reactants, the density of unbound states makes a significant contribution.

IV. MONTE CARLO METHOD

For separable degrees of freedom, excellent methods for calculating sums and densities of states have been developed, but these methods cannot be applied to nonseparable cases. For triatomic molecules, the factors in Eq. (7) might be evaluated by direct, explicit summation, but this brute force approach is untenable for larger molecules, because so many states are involved. Monte Carlo techniques offer a good solution to this problem, as shown elsewhere.[38]

In the present calculations, the quantum numbers (consistent with total energy E) for all noncritical DOF are first assigned by Monte Carlo selection (with shuffling of their order), including all couplings. First, J is specified and K is selected randomly, consistent with conservation of energy and with the condition that $|K| \leqslant J$; then the $n-1$ vibrational quantum numbers are assigned randomly, subject to conservation of energy. The remaining energy U is then assigned to the critical DOF and the dissociation energy of the critical DOF is evaluated from Eq. (8). Note that the properties of every oscillator are affected by the selections of J, K, and the other vibrational quantum numbers, according to Eq. (7). In any trial, if energy U is greater than the dissociation energy D of the critical DOF for that trial, or if the conditions expressed by Eq. (9) are not satisfied, the state is unbound.

An efficient method for Monte Carlo sampling within any arbitrary boundary has been presented elsewhere.[38] This weighted Monte Carlo method has an efficiency comparable to stratified sampling methods, and is particularly well suited to problems with complicated boundaries in hyperspace, where the volume of the sampling region is not known. For example, the sum of states is directly proportional to the sampling volume (which is unknown), but the boundaries are expressed by the spectroscopic term expression [e.g., Eq. (7)] and by Eq. (9). The final Monte Carlo expression for an integral (or summation) S using this method is written

$$S = N_{\text{tot}}^{-1} \sum_{i=1}^{g} f(\mathbf{g}) N_g / w_g, \tag{17}$$

where $f(\mathbf{g})$ is the integrand, a function of the vector of variables $\mathbf{g}$ (describing a particular point, or cell in hyperspace), N_{tot} is the total number of Monte Carlo trials, and N_g is the number of trials performed in the gth cell. The weighting factor w_g is a function of the range of the sampling variables within the sampling volume, and it is written

$$w_g = \prod_{i=1}^{s} R_i^{-1}, \tag{18}$$

where there are s variables and R_i is the range of the ith variable. For a complete description of this method, and an outline of the sampling algorithm, see Ref. 38.

To minimize complicated bookkeeping, we selected the Monte Carlo sampling region according to boundaries that approximately satisfied Eq. (9) for all except the last DOF. The sampling region is illustrated in Fig. (2a) for the coupled ν_1 and ν_3 modes in NO_2. (The actual sampling region is more complicated, since v_2 and the K quantum number must also be sampled.) Each (v_1, v_3) state is represented as a point on the $v_1 \times v_3$ plane and each state has an energy. In the figure, vibrational energy U is presented as a contour plot, a function of v_1 and v_3. From the origin, the energy rises and then exhibits a broad ridge with a col near $v_1 \approx 22$ and $v_3 \approx 9$, which is the minimum dissociation energy. Lines labeled A and B are the loci where the partial derivatives of U with respect to v_1 and v_3 are, respectively, equal to zero. States are bound when they are in the region bounded by lines A and B, and by the energy contour corresponding to the minimum dissociation energy. For higher energies, unbound states are found near the col.

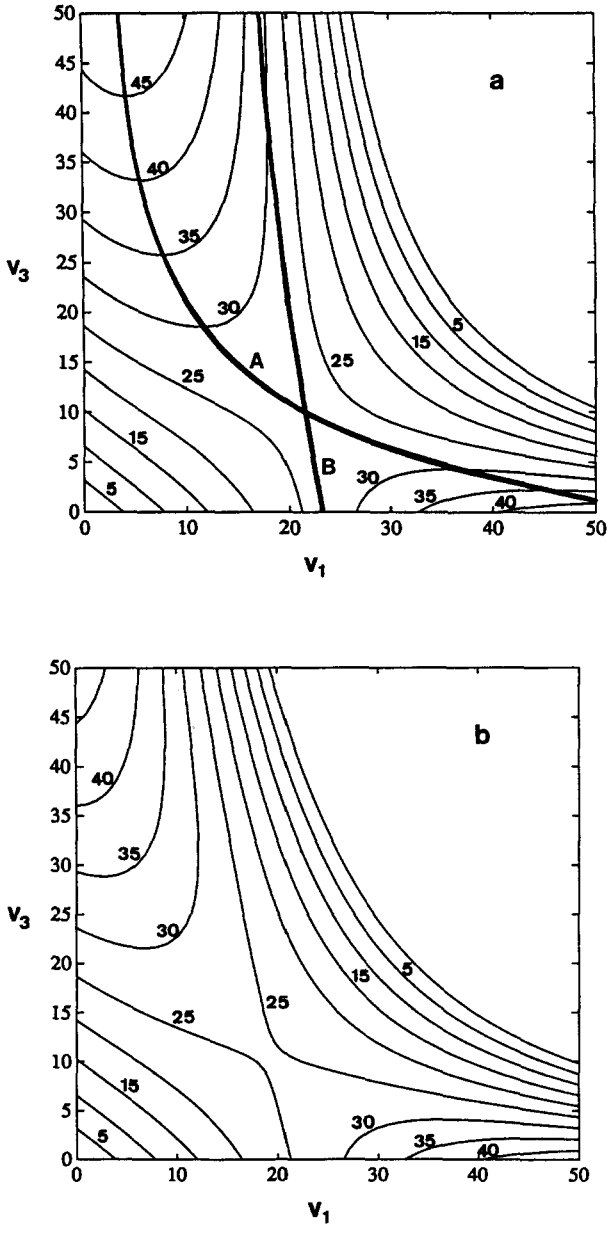

FIG. 2. Contour plots of vibrational energy as a function of vibrational quantum numbers v_1 and v_3 (thin lines). The energies (cm^{-1}) are obtained by multiplying the numbers on the lines by 1000. (a) Spectroscopic data with no adjustments: $E_c(J=0) = 26\,281\ cm^{-1}$. Lines A and B are for $\partial U/\partial v_1 = 0$ and $\partial U/\partial v_3 = 0$, respectively. (b) Adjusted spectroscopic data (with $y_{133} = -0.205$): $E_c(J=0) = 25\,132\ cm^{-1}$.

As an illustration of the boundaries, consider the molecule with 30 000 cm^{-1} of excitation energy distributed between v_1 and v_3. The maximum values for v_1 and v_3 are both ~ 23, where the former is limited by line B (i.e., $\partial U/\partial v_3 = 0$) and the latter by the energy contour. The sum of bound states with energy less than or equal to 30 000 cm^{-1} is the number of states within the area bounded by the 30 000 cm^{-1} contour and by lines A and B. The sum of states that are unbound with respect to v_3 is the length of the v_1 axis where the energy contour falls outside the boundary. For 30 000 cm^{-1}, that length is for $12 \leqslant v_1 \leqslant 23$, and therefore $G_3 \approx 11$. The corresponding sum for v_1 unbound states is $G_1 \approx 18$, and thus the total sum of unbound states is $G \approx 29$.

In every trial, $\{\mathbf{v}_{s-1}\}_i$ is selected and U is determined. If U is greater than the dissociation limit D for the last oscillator, the state is considered unbound. If U is less than D, the quantum number v_s is determined and the resulting state is tested to determine whether the conditions in Eq. (9) are satisfied. If satisfied, the state is bound, otherwise, it is unbound. The selection of the sampling boundaries minimizes the chance of inadvertantly counting states more than once that are bound in coordinate q_s, but unbound in some other coordinate.

The density of bound states is given by Eq. (13), where $\rho(U)$ is evaluated for every trial. The total density of states is given by Eq. (15). For the bound states, the densities are calculated for each vibrational mode selected separately as a possible reaction coordinate, and the final density of bound states is the average of the three separate calculations, since $N_b(E)$ should be independent of the order in which modes are selected. The summations in Eqs. (13) and (16) were evaluated in the present work according to the Monte Carlo technique just described and the accuracy of the technique for state densities was verified by comparisons with differentiated sums of states obtained using the method described in Ref. 38.

V. APPLICATION TO NO_2

The spectroscopy and unimolecular reactions of nitrogen dioxide have been studied by many investigators, providing an important test for any theory. A serious complication limits the detailed comparisons between experiment and theory, however: the experimental reaction rate determinations reflect the effects of multiple PESs, while the predictions are restricted to a single surface. The importance of this effect is estimated below.

A. Rate constant data

The unimolecular dissociation reaction of NO_2 has been investigated with shock tube techniques at high temperatures in the low pressure region and over much of the fall-off.[50]

$$NO_2(^2A_1) \rightarrow O(^3P) + NO(^2\Pi). \qquad (19)$$

The recombination reaction has been studied by several techniques in the low pressure limit over a range of lower temperatures.[51,52] Quantum yield measurements[53] at very high pressure have been used to determine the recombination rate constant relative to the well known rate constant for reaction (20)[54]:

$$O(^3P) + NO_2 \rightarrow O_2 + NO. \quad (20)$$

Other quantum yield measurements were subjected to a Stern–Volmer analysis to derive values for $k(E)$ that are uncertain by about a factor of two.[55] In addition, photofragmentation spectroscopy provides an estimate for the lower limit $k(E,J) > 5\times10^{-12}$ s^{-1} at a photon energy of 28 810 cm^{-1}.[56] The equilibrium constant for the reaction is well known,[57] providing a solid connection between the dissociation and recombination kinetics experimental data. These kinetics and thermochemical data constitute one of the most complete data sets available for any unimolecular reaction system.

B. Spectroscopic data

1. Data set

A very extensive set of spectroscopic constants has been determined for NO_2, as presented in Table I. All of the vibrational frequencies, quadratic anharmonicities, and a few of the cubic anharmonicities for NO_2 have been determined. The differences among the determinations of the cubic anharmonicities are mostly due to different ways of treating the Darling–Dennison perturbations. (Darling–Dennison and other perturbations could be considered explicitly in the calculations described here, but for present purposes they are neglected.) The rotational constants, centrifugal stretching coefficients, and the rovibrational coupling coefficients have been determined to high order, and the dissociation energy is well known.

The spectroscopic constants determined by Sams and Lafferty[30,58] were adopted for the calculations, except for the four cubic vibrational anharmonicities y_{ijk}, which were taken from Bist and Brand.[29] This approach was taken because Sams and Lafferty explicitly included Darling–Dennison couplings in their treatment, while Bist and Brand's treatment absorbed the effects of the coupling within the cubic anharmonicities. Rather than add more complexity to the calculation, we used Bist and Brand's cubic terms.

2. Problems with extrapolations

The spectroscopic data were obtained at relatively low energies and the molecular constants were determined for the usual power law expansions in terms of the vibrational and rotational quantum numbers, as in Eq. (7). Clearly, there is the real danger that the use of such expressions will be completely inadequate for predicting the energies of highly excited states. For the power law expansions to converge, enough terms must be included so that the high order terms are much smaller in magnitude than the low order terms. Unfortunately, the spectroscopic data are seldom extensive enough to include the needed terms. This problem manifests itself in the present data set by an inconsistency between the vibrational parameters and the dissociation energy. It is also evident in divergent rotational terms for large values of the rotational quantum numbers.

3. Vibrational parameters and dissociation energy

In this work, the exact positions of the excited states are less important than the average densities of states and the

TABLE I. NO_2 spectroscopic constants[a] (in cm^{-1}).

ω_1^e	1325.325			γ_{22}^{0A}	0.014 33
ω_2^e	750.141			γ_{33}^{0A}	3.74(− 3)
ω_3^e	1633.860			γ_{12}^{0A}	0.030 9
X_{11}	− 5.471			γ_{13}^{0A}	− 0.014 0
X_{22}	− 0.469			γ_{23}^{0A}	− 0.020 3
X_{33}	− 17.062			β_1	− 2.09(− 4)
X_{12}	− 6.433			β_2	− 8.66(− 4)
X_{13}	− 29.549			β_3	2.34(− 4)
X_{23}	− 11.399			A_0	8.001 15
y_{111}	···	− 0.07[b]		B_0	0.433 637
y_{333}	0.068	0.07[b]		C_0	0.410 398
y_{133}	− 1.146	0.34[b]	− 0.205[c]	Δ_J	3.006 8(− 7)
y_{113}	···	− 1.75[b]		Δ_{JK}	− 1.949 9(− 5)
α_1^{0A}	− 0.0835			Δ_K	2.688 1(− 3)
α_2^{0A}	− 0.3577			H_J	5.3(− 13)
α_3^{0A}	0.2313			H_{JK}	− 3.7(− 10)
α_1^{0B}	2.45(− 3)			H_{KJ}	1.97(− 8)
α_2^{0B}	4.82(− 4)			H_K	2.946 1(− 6)
α_3^{0B}	2.707 − 3)			L_K	3.55(− 9)
γ_{11}^{0A}	0.0038			D(ON–O)	25 132[d]

[a] From Refs. 27 and 58 unless otherwise noted. Numbers in parentheses indicate power of 10, i.e., 3.0(− 4) is 3.0×10^{-4}.
[b] Reference 26.
[c] Adjusted in present work; see the text for details.
[d] Reference 28.

sums of unbound states, except for the location of the dissociation energy, which strongly influences reaction kinetics.

The dissociation energy predicted by the spectroscopic constants was determined by using Monte Carlo selection of the $s-1$ quantum numbers in Eq. (7) with the spectroscopic data in Table I. Numerous trials were carried out; in each trial, the binding energy of the critical Morse oscillator depends on $\{v\}_{s-1}$ and the dissociation energy (measured from the zero point energy) for each trial is the binding energy D summed with E_{s-1}, which includes the rotational energy, if any. The minimum such dissociation energy (measured from the reactant zero point energy for $J=0$) is identified with the reaction critical energy $E_c(J)$ for the specified J state.

For $J=0$ and for no adjustments of the spectroscopic data, the reaction critical energy was found to be 26 281 cm^{-1}, which is only 1149 cm^{-1} higher than the known dissociation energy. Considering the extrapolations involved, this agreement is exceptionally good, but the discrepancy reveals the importance of the unknown high order spectroscopic constants.

An empirical method was used to reconcile the data. In the "cubic" method, the cubic anharmonicity y_{133} was adjusted (see Table I) to give the known dissociation threshold energy $E_c(J=0)=25\ 132\ cm^{-1}$. This method does little violence to the low energy spectroscopic data and has relatively little effect on the coupling between modes 1 and 3, as evidenced by the similarity of the two panels in Fig. 2. The first panel in Fig. 2 shows the vibrational energy as a function of v_1 and v_3 obtained using the original unadjusted data set. The crest of the broad "ridge" that extends from upper left to lower right is the dissociation energy as a function of the two quantum numbers. The lowest point along the ridge is the dissociation threshold. Note that the minimum dissociation energy is achieved only when *both* ν_1 and ν_3 are excited. Other combinations of these two quantum numbers may have nearly the same energy, but the reactant will not dissociate. Figure 2(b) is similar to panel (a), but here the adjusted data were used. It is noteworthy that the general features of Figs. 2(a) and (b) are very similar, except for the dissociation energy. This indicates that the intermode coupling between ν_1 and ν_3 are quite similar in both cases.

4. Problems with rotational constants

The rotational constants for NO_2 are based on states at relatively low energies ($\sim 8500\ cm^{-1}$), but the rotational constants are exceptionally complete. For reactions at 1500 K, $k(E,J)$ values for J up to ~ 100 are needed. Unfortunately, the known rotational constants are not well-behaved for extrapolations to high energies, because the high order terms are not sufficiently small for the power series expansion to converge.

Watson[40] and others have discussed the convergence criteria for the rotational constants and it has been concluded that each successive set of higher order terms must be $<10^{-4}$ times the preceding order. Thus, L_K should be $<10^{-4}\times H_K$, etc. Although some molecules satisfy this condition,[59] NO_2 does not, and the rotational energy expression does not converge for high values of J and K. To avoid this problem in the present work, we neglected terms in K and terms in $J(J+1)$ that are higher order than quadratic. Results from our calculations using all terms are indistinguishable from those that use just the low order terms, for J's less than ~ 20, where the power series is still convergent. For higher J's, the full expression cannot be used and we are forced to neglect the higher order terms.

This solution to the nonconvergence problem is not very satisfactory, because most of the rotational energy is not available for redistribution among the other DOF and a miscalculation directly affects the reaction rate constants. Unfortunately, we are limited to the known spectroscopic data and must neglect the higher order terms, until a spectroscopic term expression is found that converges faster.

C. Effects of electronically excited states

To compare theory with experiment, the effects of electronically excited states must be estimated and the theoretical rate constant multiplied by correction factor β_e^T, or $\beta_e(E)$ for thermal and microcanonical rate constants, respectively. Smith[34] has described a method for estimating β_e^T for recombination rates, when the electronic states are not coupled. Essentially, each individual electronic state has an associated falloff curve. If electronic quenching of the vibrationally stabilized electronically excited molecules is faster than redissociation, the excited electronic state makes a contribution to the overall reaction, otherwise it is unimportant. Smith used Troe's methods[15] to calculate the low pressure rate constants (assuming a collision efficiency $\beta_c \approx 0.2$ for all electronic states in collisions with argon) and the maximum free energy model of Quack and Troe[60] to calculate the high pressure rate constants for the recombination of NO + O to form NO_2. He concluded that at 300 K k_0 and k_∞ are increased by factors of $\beta_e^T(0)\approx 1.7$ and $\beta_e^T(\infty)\approx 2.9$, respectively, due to contributions from electronically excited states.

We have repeated Smith's calculations[34] on NO_2 for a wide range of temperatures using his input parameters, which were derived from a theoretical calculation,[61] we obtained results similar to Smith's: there is very little temperature dependence over the range form 200 to 2000 K and the correction factors for the low and high pressure limits are ~ 1.5 and ~ 3.5, respectively.

In Smith's approach, the electronic states are assumed to be separable in the isolated molecules. However, it is known that at least two of the three excited states in NO_2 undergo rapid internal conversion and it seems likely that strong coupling with the ground state exists for all three excited states.[32,62] If the coupling is very strong and rapid, every vibrational level of every electronic state will be perturbed in energy and also will contribute equally (statistically) to the density of states (both bound and unbound) and the sum of reactive states (if unbound). Thus the density and the sum of vibrational states are sums of the contributions from the individual electronic states. For the purpose of state counting, we can neglect the energy perturbations and assume that the vibrations and rotations are separable. For the four electronic states that are assumed to be coupled in NO_2, the total density and sum of states are given by

$$N_T(E) = \sum_i N_i(E - T_i)h(E - T_i) \quad (21)$$

$$G_T(E) = \sum_i G_i(E - T_i)h(E - T_i), \quad (22)$$

where the summations are over the contributing electronic states, and $N_i(E)$ and $G_i(E)$ are the density and sum of vibrational states, respectively, for each electronic state. The Heaviside step functions $h(E - T_i)$ are zero for energies less than the electronic state origins at energies T_i, and unity above.

To estimate crudely the effects of electronic states, we applied RRKM theory in a simplified way. Specifically, we used the vibrational frequencies and energy origins T_i tabulated by Smith[34] for each electronic state of NO_2 and used the Stein–Rabinovitch algorithm[63] to calculate the corresponding densities of states that appear in Eq. (21). The bending modes were assumed to be harmonic oscillators and the stretching modes were treated as Morse oscillators with dissociation energy given by $D_i(\text{cm}^{-1}) = 25\,132 - T_i$ for each electronic state. The transition states for reaction were crudely assumed to have the same frequencies for reaction as the electronic states themselves, except the symmetric stretch mode was assumed to be the reaction coordinate in each case. This crude approach is justified only because the transition states for the excited electronic states are unknown and must be guessed, in any event. The total sum of states $G_T^{\ddagger}(E)$ for the transition state(s) was calculated according to Eq. (22) by the Stein–Rabinovitch algorithm. The correction factor for the specific rate constants (i.e., $k(E)$'s] is then the ratio of the total RRKM rate constant to that for the ground state ($i = 0$):

$$\beta_e(E) = \frac{G_T^{\ddagger}(E)}{N_T(E)} \frac{N_0(E)}{G_0^{\ddagger}(E)}. \quad (23)$$

The crude assignment for the transition state gave a ground state absolute rate constant that is about a factor of 10 too low, but it is assumed that the relative effects of the electronic states according to Eq. (23) are still estimated with sufficient accuracy. This correction factor according to Eq. (23) was found to be ~ 1.7 for energies up to $\sim 35\,000$ cm^{-1}. The corresponding high pressure and low pressure limiting thermal correction factors (300 K) were found to be $\beta_e^T(0) \approx 2.8$ and $\beta_e^T(\infty) \approx 4.5$, respectively, only a little higher than those found using Smith's method. Clearly, better methods for estimation of this factor must be developed in future work.

D. Thermal rate constants

In general, it is desirable to use the densities of states [$N(E,J)$'s] and specific rate constants [$k(E,J)$'s] in a full Master Equation treatment of the reaction system, whether thermal, or nonthermal.[64,65] For present purposes, this procedure is not justified because the collisional energy transfer parameters are unknown and the calculation is too cumbersome. The limiting high pressure unimolecular rate constant is independent of energy transfer parameters and can be calculated directly:

$$k_\infty(T) = \beta_e^T(\infty)Q^{-1}h^{-1}\sum_J (2J+1) \times \int_{E_c(J)}^{\infty} G(E,J)\exp(-E/kT)dE. \quad (24)$$

In this expression, E is the total energy, Q is the rovibrational partition function at temperature T, and the effects of excited electronic states are reflected in $\beta_e^T(\infty)$.

The intermediate and low pressure rate constants depend on energy transfer parameters, which are unknown for NO_2. Nevertheless, the "strong collision" low pressure rate constant can be calculated directly:

$$k_0^{\text{sc}}(T) = \beta_e^T(0)Q^{-1}Z_{\text{LJ}}\sum_J (2J+1) \times \int_{E_c(J)}^{\infty} N(E,J)\exp(-E/kT)dE \quad (25a)$$

$$k_0(T) = \beta_c k_0^{\text{sc}}(T), \quad (25b)$$

where β_c is the (unknown) collision efficiency, Z_{LJ} is the Lennard-Jones collision rate constant, and $k_0(T)$ is the weak collider low pressure rate constant. Rate constants for the recombination reaction are obtained through use of the equilibrium constant.

E. Results

The densities of NO_2 bound states calculated according to the present method are compared in Fig. 3 to state densities calculated according to two other methods. As shown elsewhere,[38] Monte Carlo calculation of the sum of states can include all couplings among the degrees of freedom and therefore gives the exact result, but the Stein–Rabinovitch method can be applied only for separable degrees of freedom. The exact density of states was determined by fitting the sums of states from the Monte Carlo method to a polynomial and then taking the derivative. Figure 3 shows that the Stein–Rabinovitch method underestimates the density of bound states by 40% near the dissociation energy and the error increases significantly at higher energies. The semiclassical Monte Carlo method used here for calculating densities of bound states gives results that are correct to within about 10% for the entire energy range, demonstrating its utility for nonseparable anharmonic degrees of freedom.

Above the reaction threshold, unbound states make an important contribution to the total density of states, as shown in Fig. 4. At still higher energies, $N_b(E)$ decreases to zero and all states are unbound. The incorporation of $N_u(E)$ is different from usual applications of RRKM theory, SACM, and other statistical theories which neglect the unbound states. The unbound states must be included in calculations involving triatomics, since their omission can lead to significant errors, especially at higher energies. However, for molecules larger than triatomics at moderate energies, the contribution of the unbound states can be neglected safely, for most purposes.[45]

The sum of unbound states (open channels) $G(E,J)$ can be compared with results obtained using the SACM and the Wardlaw–Marcus[49] RRKM Theory. Figure 5 is adapted from the work of Wardlaw and Marcus, where they showed

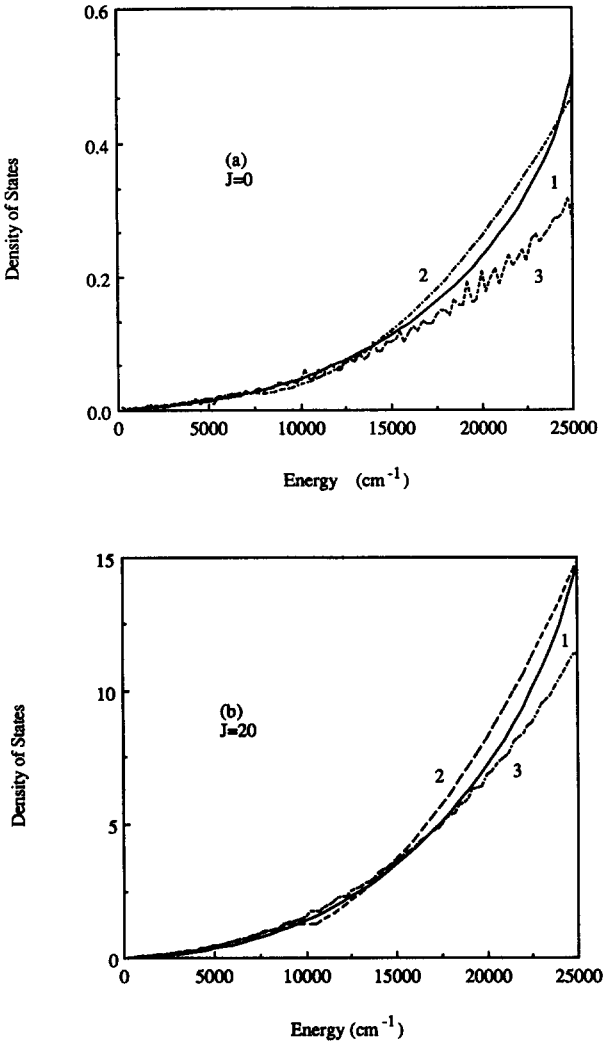

FIG. 3. Density of bound states vs total energy for $J = 0$ and 20 using three different methods of calculation and spectroscopic data from Table I. (1) Semiclassical method presented in this work [Eq. (11)]. (2) Full density of states derived from Monte Carlo sum of states including all spectroscopic terms in Eq. (7) (method of Ref. 38). (3) Separable degrees of freedom, according to Stein–Rabinovitch (Ref. 63) method.

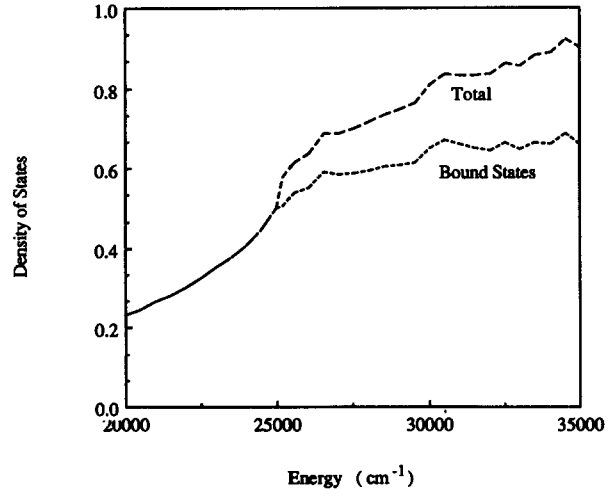

FIG. 4. Total density of states and density of bound states, for $J = 0$, calculated with present method and spectroscopic data from Table I. Note the important contribution from the unbound states.

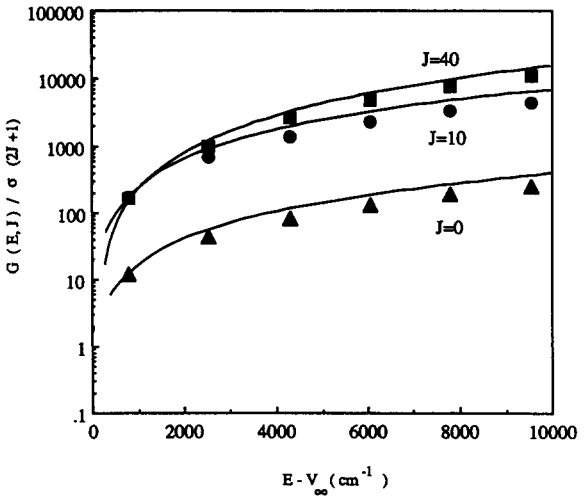

FIG. 5. Sums of reactive states (open channels) according to the Wardlaw and Marcus (Ref. 49) (symbols) and the present approach (solid lines) for $J = 0$, 10, and 40.

the close agreement between their extension of RRKM theory for a particular model PES and results obtained using the SACM.[18] The values obtained for $G(E,J)$ obtained in the present work are in excellent agreement with the other approaches. The present results are based on experimental data for high-order spectroscopic properties of NO_2, while the other approaches employ an empirical PES (which is also partly based on NO_2 spectroscopic data). It is gratifying that the three independent approaches to this problem have produced such consistent results. The close agreement between the three methods indicates that $k(E,J)$'s from all three methods are very similar, when the same densities of states are used. (However, the other approaches do not use the same densities of states, since they neglect intermode coupling.) The resulting thermal rate constants will also be very similar, except at low temperatures, where small threshold energy differences may become important.

Using the density of states and the sum of unbound states at each energy, $k(E,J)$ was calculated according to Eq. (1); a sufficient number of Monte Carlo trials was performed so that the $k(E,J)$ values had about $\pm$ 5% statistical uncertainty, as shown by the error bars in Fig. 6. The calculated $k(E,J)$ values presented in Fig. 6 superficially resemble those obtained using the SACM.[18] Wardlaw and Marcus[49] did not actually calculate rate constants and a direct comparison with their work is not possible. A close inspection shows that the threshold energies predicted from the spectroscopic data in the present work do not correspond exactly with those of the SACM, but this difference is not large (Wardlaw and Marcus did not report threshold energies). The threshold energies are very important for thermal rate constants at low temperatures, as discussed below.

In Fig. 7, the comparison between predicted $\beta_e(E) \times k(E,J=0)$ and experimental values for $k(E)$ shows excellent agreement. The experimental values have an estimated uncertainty of a factor of 2 and *the predicted values are based exclusively on spectroscopic data, with no fitting of kinetics results.*

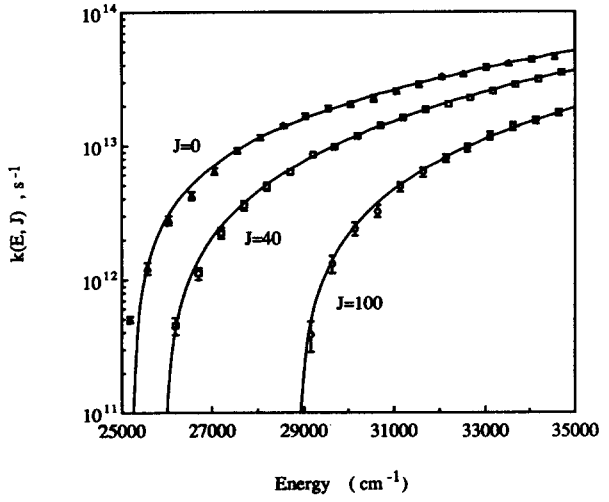

FIG. 6. Specific rate constants $k(E,J)$, according to Eq. (1) for the "cubic method" (see the text for details). The error bars represent the Monte Carlo statistical uncertainty.

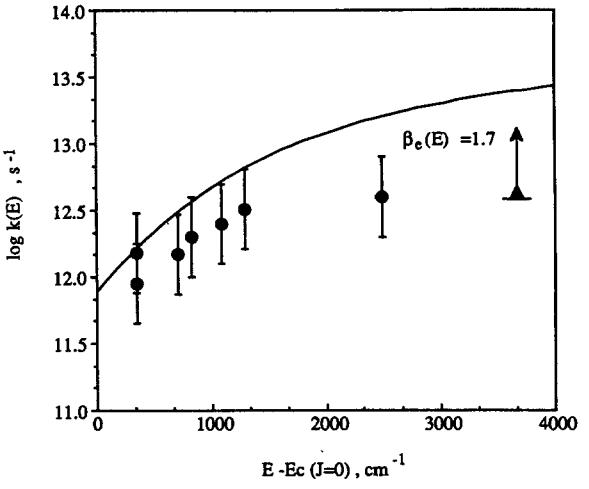

FIG. 7. Experimental (symbols) and predicted values (solid lines) of $k(E)$. The solid line represents $\beta_e(E)\times k(E,J=0)$, with $\beta_e(E)=1.7$ (see the text). (○) Experimental $k(E)$ from Ref. 55 (factor of 2 uncertainty) (△) Experimental $k(E)$ lower limit from Ref. 56.

Values for the high pressure limiting thermal rate constants were obtained by numerical integration of Eq. (24). For convenience, all of the results for $N(E,J)$, $G(E-E_c,J)$, $k(E-E_c,J)$, and $E_c(J)$ were least-squares fitted to polynomials using multiple regression (Table II). For thermal systems at $T\leqslant 2000$ K, most of the contribution to the partition functions comes from low energies of excitation, where coupling among the DOF can be neglected. Thus the partition functions were calculated using standard formulas,[66] which were checked for accuracy in a few cases by numerical integration using densities of states calculated with the Stein–Rabinovitch method.

According to the RSM, the high pressure thermal rate constant for dissociation, including the factor $\beta_e^T(\infty)$, was found to be $k_\infty^{\mathrm{RSM}}(T)=2.09\times10^{15}(T/300)^{0.6}\times\exp(-36\,503/T)\ \mathrm{s}^{-1}$. Thermal rate constants at the high pressure limit provide a test of the theoretical predictions of $G(E)$, but the experimental high pressure limit can only be obtained by uncertain extrapolation of experimental falloff curves. The effects of electronically excited states also introduce uncertainties. Nonetheless, the predicted rate constant compares very well over the whole range of experimental temperatures with the experimental high pressure rate constant,[50] $k_\infty(T)=2.0\times10^{14}\exp(-36\,198/T)\ \mathrm{s}^{-1}$, which is uncertain by at least a factor of 2.

Although the agreement between prediction and experiment is excellent, the minor difference in temperature dependence could be eliminated by slight changes in the $E_c(J)$ threshold energies for higher J states. These threshold energies depend on the coupling between rotations and vibra-

TABLE II. Least squares fits to calculated factors.[a]

$$\ln[Y(X,J)]=A+B\ln(X)+C[\ln(X)]^2+D[\ln(X)]^3+E\ln(J+1)+F[\ln(J+1)]^2+G[\ln(J+1)]^3+H\{\ln(X)\times\ln(J+1)\}+L\ln(X)\times[\ln(J+1)]^2+M\{[\ln(X)^2\times[\ln(J+1)]^2\}+P\{[\ln(X)^3\times[\ln(J+1)]\}$$

$$E_c(J)=A+BJ+CJ^2$$

	$Y(X,J)$: $N(E,J=0$–$100)$	$h^{-1}G(E-E_c,J)$	$k(E-E_c,J)$	$E_c(J)$
A	−8.585(3)	3.124(1)	3.167(1)	25 132
B	2.476(3)	−2.701	−2.686	0.253
C	−2.382(2)	0.434	0.443	0.347
D	7.638	−0.015	−0.0165	
E	−3.745(1)	0	−1.491	
F	−0.703	0	0	
G	−0.029	0	0.034	
H	5.703	0.297	0.326	
L	0.0707	−0.067	−0.0708	
M	0	0.0049	0.0046	
P	−0.018	−0.0013	−0.0014	

[a] $X=E$ for column 2, $X=(E-E_c)$ for columns 3 and 4.

tions, which are expressed in Eq. (7) by terms up to fourth order in K and by terms up to only second order in v_i and in J. Since the spectroscopic data fits only included vibrational assignments up to about 8500 cm^{-1} and J, K levels up to ~ 40, the extrapolations to higher J levels and higher energies are very long, possibly leading to the $\sim 300\ cm^{-1}$ shifts in $E_c(J)$ for higher J that may account for the discrepancies between predictions and experiment. Alternatively, the slight difference may be due to our crude estimate of the effect of excited electronic states.

Recombination rate constants k_{rec} are not calculated directly in the present work, but are determined by their relationship with the calculated dissociation rate constant and the equilibrium constant: $k_{rec}(T) = k(T)/K_{eq}$. In the present work, K_{eq} was calculated using the JANAF Tables.[57] Low pressure limit recombination rate constants depend on the strong-collider rate constant k_0^{sc} and on the collision efficiency β_c, which is not known independently of theory for NO_2: $k_0(T) = \beta_c(T) k_0^{sc}(T)$. The strong-collider recombination rate constant at low temperature was determined from numerical integration of Eq. (25) to be $k_{rec,0}^{RSM} = 2.4 \times 10^{-32} (T/300)^{-0.42}\ cm^6\ s^{-1}$, which can be compared with the experimental value[67] for argon collider gas: $k_{rec,0} = 6.8 \times 10^{-32} (T/300)^{-1.86}$. The temperature dependence of the calculated weak collider recombination rate constant will include that of β_c (i.e., $\sim T^{-1}$), producing an overall temperature dependence of $\sim T^{-1.42}$, which is slightly smaller than that observed.

Near 300 K, the calculated rate constant is significantly lower than the experimental value even before multiplication by β_c, which must be less than unity, but at higher temperatures, the discrepancy disappears. Considering that β_c is expected to be $\leqslant 0.3$, the calculated rate constant at 300 K is probably at least a factor of 10 too low. This discrepancy may be due to several factors: (1) a small error in the predicted thresholds for reaction $E_c(J)$ can give low rate constants, especially at low temperature; (2) possible underestimates of the extent of rovibrational coupling near the reaction threshold can lead to an underestimate of state density and low rate constants; and (3) errors in our crude estimate of β_e^T can lead to a low predicted rate constant. The first possible explanation arises because the low temperature recombination rate constant was calculated from the dissociation reaction and the equilibrium constant. Although the threshold energy for $J = 0$ is known exactly, the corresponding thresholds for the higher J values important at 300 K are only known approximately from spectroscopic data. Changes in the coupling between rotation and vibration can change the higher J thresholds and will affect the thermal rate constants. The second and third possible explanations may be inextricably intertwined, since the presence of excited electronic states may affect rovibrational coupling within any "single" electronic state.[32] Both effects will lead to higher densities of states, but they will also lead to higher sums of states, which would diminish the excellent agreement with the experimental high pressure limit. Development of better methods for estimating β_e^T deserves high priority, since excited electronic states may be important in many (even most) recombination reactions.

VI. CONCLUSIONS

Conceptually, the present theory is closely related to RRKM theory and the statistical adiabatic channel model. The most important new feature of this theory is that a single set of high order spectroscopic data is used as the basis for calculating both sums of reactive states and densities of molecular states. This has the clear conceptual advantage over conventional applications of RRKM theory in that each reactive unbound state is also a molecular state and must contribute to the total density of states. In conventional applications of RRKM theory, the reactant and the transition state have separate state assignments and the energies of these separate sets of states usually do not coincide.

In the SACM, the unbound states (open channels) connect molecular states to product states according to empirical, or calculated potential energy curves. (Thus, the unbound sates should also contribute to the total density of states, although their contribution heretofore has been neglected.) The present approach is similar, except that instead of potential curves and approximate coupling terms, the spectroscopic data are used directly to calculate sums and densities of states for nonseparable anharmonic modes. Moreover, the adiabatic correlations with product states in the SACM are not necessary in the present model. The present theory is more like RRKM theory in this regard, since the product states play no role in determining the theoretical rate constant. By adding an adiabatic assumption,[68] however, the present theory might be extended to predict product state distributions; future work will explore this possibility.

High-order spectroscopic data are used in the present theory, including intermode and rovibrational coupling terms. These terms add substantially to the realism of the present calculations, but they also necessitate the use of Monte Carlo techniques. The additional calculational effort is not large, however: the calculations reported here were performed using a Macintosh II microcomputer. More realistic theories use Hamiltonians derived from the spectroscopic data,[69] but inversion of the spectroscopic data to obtain the PES is not easy. The present theory avoids this difficult step and still retains virtually all of the information carried by the spectroscopic data.

Equation (1) applies to dissociation reactions, where a true continuum exists. In isomerization reactions, all states are bound, and special care must be taken to account properly for this fact.[70] It seems quite feasible to extend the basic ideas in the present model to such reactions.

Some empiricism has been necessary in implementing the present theory, because the known dissociation limit does not agree with extrapolation of the low energy spectroscopic data. This sort of discrepancy is familiar from Birge–Sponer extrapolations to dissociation limits in diatomic molecules and is due to the omission of higher-order anharmonicities, which are usually unknown. To compensate for this discrepancy, an empirical method was introduced and the results were shown to agree very well with other theories and with experimental data. Although we have made no attempt to fit the theory to experiment, such fitting in principle can be carried out very successfully by empirically adjusting the

unknown high-order spectroscopic parameters. It is worth noting that spectroscopic Hamiltonians that depend on polynomial expansions are not particularly suitable for extrapolations to high quantum numbers; the development of other functional forms is most desirable.

The predicted thermal rate constants reported here for NO_2 are in moderate agreement with the experimental data. There is, however, a major source of uncertainty in making comparisons with the experiments: the role of electronically excited states. Nevertheless, even with crude estimates for this effect, the theoretical predictions are in reasonable agreement with experiment, showing that this approach has great promise in interpreting, fitting, and predicting unimolecular reaction rate data when appropriate spectroscopic, or theoretical data are available.

ACKNOWLEDGMENTS

Thanks go to R. G. Gilbert, J. Troe, W. L. Hase, and J. M. Bowman for helpful discussions, to D. M. Wardlaw for providing the numerical data in Fig. 5, and to a referee for some very useful comments. B. M. T. thanks CONICET of Argentina for a postdoctoral fellowship. This research was funded in part by the U. S. Department of Energy, Office of Basic Energy Sciences.

[1]For a recent review, see D. G. Truhlar, W. L. Hase, and J. T. Hynes, J. Phys. Chem. **87**, 2664 (1983).
[2]P. J. Robinson and K. A. Holbrook, *Unimolecular Reactions* (Wiley-Interscience, London, 1972).
[3]W. Forst, *Theory of Unimolecular Reaction* (Academic, New York, 1973).
[4]F. A. Lindemann, Trans. Faraday Soc. **17**, 599 (1922).
[5](a) R. A. Marcus and O. K. Rice, J. Phys. Colloid. Chem. **55**, 894 (1951); (b) R. A. Marcus, J. Chem. Phys. **20**, 359 (1952); (c) G. M. Wieder and R. A. Marcus, *ibid.* **37**, 1835 (1962). (d) R. A. Marcus, *ibid.*, **43**, 2658 (1965).
[6]J. D. Rynbrandt and B. S. Rabinovitch, J. Phys. Chem. **74**, 4175 (1970); **75**, 2164 (1971).
[7]V. E. Bondybey, Annu. Rev. Phys. Chem. **35**, 591 (1984).
[8]F. F. Crim, Annu. Rev. Phys. Chem. **35**, 657 (1984).
[9]D. L. Bunker and M. Pattengill, J. Chem. Phys. **48**, 772 (1968).
[10]D. W Noid, M. L. Koszykowski, and R. A. Marcus, Annu. Rev. Phys. Chem. **32**, 267 (1981).
[11]K. N. Swamy, W. L. Hase, B. C Garrett, C. W. McCurdy, and J. F. McNutt, J. Phys. Chem. **90**, 3517 (1986).
[12]T. Uzer and J. T. Hynes, J. Phys. Chem. **90**, 3524 (1986).
[13]J. Troe, J. Chem. Phys. **66**, 4745, 4758 (1977).
[14]S. W. Benson *Thermochemical Kinetics*, 2nd ed. (Wiley, New York, 1976).
[15]J. Troe, J. Phys. Chem. **83**, 114 (1979).
[16]P. Pechukas and J. C. Light, J. Chem. Phys. **42**, 3281 (1965); J. C. Light, Discuss. Faraday Soc. **44**, 14 (1967); C. E. Klots, J. Phys. Chem. **75**, 1526 (1971).
[17]Also see C. Wittig, I. Nadler, M. Noble, J. Catanzarite, and G. Radhakrishnan, J. Chem. Phys. **83**, 5581 (1985).
[18]M. Quack and J. Troe, Ber. Bunsenges. Phys. Chem. **78**, 240 (1973); **79**, 170, 469 (1975); J. Troe, J. Chem. Phys. **75**, 226 (1981); **79**, 6017 (1983).
[19]J. Troe, J. Chem. Phys. **87**, 2773 (1987).
[20]N. B. Slater, *Theory of Unimolecular Reactions* (Cornell University, Ithaca, NY, 1959).
[21]H. O. Pritchard, *The Quantum Theory of Unimolecular Reactions* (Cambridge University, Cambridge, 1984). Also see H. O. Pritchard, J. Phys. Chem. **89**, 3970 (1985); **90**, 4471 (1986).
[22]P. Pechukas, in *Dynamics of Molecular Collisions, Part B*, edited by W. H. Miller (Plenum, New York, 1976), p. 269.
[23]O. K. Rice, J. Phys. Chem. **65**, 1588 (1961).
[24]R. D. Levine, *Quantum Theory of Molecular Rate Processes* (Oxford University, Oxford, 1969), Chap. 3.5.
[25]W. H. Miller, J. Chem. Phys. **61**, 1823 (1974); Acc. Chem. Res. **9**, 306 (1976).
[26]Also see W. L. Hase, Acc. Chem. Res. **16**, 258 (1983).
[27]W. H. Miller, J. Chem. Phys. **65**, 2216 (1976).
[28]For example, see D. A. Clabo, Jr., W. D. Allen, D. B. Remington, Y. Yamaguchi, and H. F. Schaefer III, Chem. Phys. **123**, 187 (1988).
[29]H. D. Bist and J. C. D. Brand, J. Mol. Spectrosc. **62**, 60 (1976).
[30]W. J. Lafferty and R. L. Sams, J. Mol. Spectrosc. **66**, 478 (1977).
[31]E. A. Douglas and K. P. Huber, Can. J. Phys. **43**, 74 (1965); W. M. Uselman and E. K. C. Lee, J. Chem. Phys. **64**, 3457 (1976).
[32]A. E. Douglas, J. Chem. Phys. **45**, 1007 (1966); J. L. Hardwick and W. J. Lafferty, J. Mol. Spectrosc. **100**, 358 (1983).
[33]For a succinct summary, see D. K. Hsu, D. L. Monts, and R. N. Zare, *Spectral Atlas of Nitrogen Dioxide 5530 to 6480 Å* (Academic, New York, 1978), 46ff.
[34]I. W. M. Smith, Int. J. Chem. Kinet. **16**, 423 (1984).
[35]For a discussion of one-dimensional unimolecular rate thoery, see P. H. Crib, S. Nordholm, and N. S. Hush, Chem. Phys. **29**, 43 (1978).
[36]For example, see stimulated emission pumping spectra such as those reported by J. P. Pique, Y. M. Engel, R. D. Levine, Y. Chen, R. W. Field, and J. L. Kinsey, J. Chem. Phys. **88**, 5972 (1988) and references therein.
[37]R. J. LeRoy and W.-H. Lam, Chem. Phys. Lett. **71**, 544 (1980); R. J. LeRoy, in *Semiclassical Methods in Molecular Scattering and Spectroscopy*, edited by M. S. Child (Reidel, Dordrecht, 1980), p. 109; J. W. Tromp and R. J. LeRoy, Can. J. Phys. **60**, 26 (1982).
[38]J. R. Barker, J. Phys. Chem. **91**, 3849 (1987).
[39]L. D. Landau and E. M. Lifshitz, *Quantum Mechanics* (Pergamon, Oxford, 1965), p. 71 and 72.
[40]J. K. G. Watson, J. Chem. Phys. **46**, 1935 (1967); **48**, 4517 (1968); M. R. Aliev and J. K. G. Watson, in *Molecular Spectroscopy: Modern Research, Vol. III*, edited by N. Rao (Academic, Orlando, FL 1985), p. 1.
[41]J. C. Keck. Adv. Chem. Phys. **13**, 85 (1967).
[42]This is closely related to the Bohr–Sommerfeld quantization rule; see A. Messiah, *Quantum Mechanics* (Wiley, New York, 1968), Vol. 1, 34ff.
[43]Called the "boxed oscillator" by I. Rusinek and R. E. Roberts, J. Chem. Phys. **68**, 1147 (1978).
[44]For thermodydnamic properties of this model, see F. H. Mies and P. S. Julienne, J. Chem. Phys. **77**, 6162 (1982).
[45]B. M. Toselli and J. R. Barker (unpublished calculations).
[46]E. Pollak and P. Pechukas, J. Am. Chem. Soc. **100**, 2984 (1978).
[47]D. R. Coulson, J. Am. Chem. Soc. **100**, 2992 (1978).
[48]For example, R. Viswanathan, L. M. Raff, and D. L. Thompson, J. Chem. Phys. **81**, 828 (1984).
[49]D. M. Wardlaw and R. A. Marcus, Chem. Phys. Lett. **110**, 230 (1984); D. M. Wardlaw and R. A. Marcus, J. Chem. Phys. **83**, 3462 (1985).
[50]J. Troe, Ber. Bunsenges. Phys. Chem. **73**, 144 (1969).
[51]J. V. Michael, W. A. Payne, and D. A. Whytock, J. Chem. Phys. **65**, 4830 (1976).
[52]M. Schieferstein, K. Kohse-Höinghaus, and F. Stuhl, Ber. Bunsenges. Phys. Chem. **87**, 361 (1983).
[53]J. Troe, Ber. Bunsenges, Phys. Chem. **73**, 906 (1969).
[54]W. D. DeMore, M. J. Molina, S. P. Sander, D. M. Golden, R. F. Hampson, M. J. Kurylo, C. J. Howard, and A. R. Ravishankara, NASA/JPL Publication No. 87-41, 1987.
[55]H. Gaedtke, H. Hippler, and J. Troe, Chem. Phys. Lett. **16**, 177 (1972); Von H. Gaedtke and J. Troe, Ber. Bunsenges. Phys. Chem. **77**, 24 (1973); **79**, 184 (1975).
[56]G. E. Busch and K. R. Wilson, J. Chem. Phys. **56**, 3638 (1972).
[57]M. W. Chase, Jr., C. A. Davies, J. R. Downey, Jr., D. J. Frurip, R. A. McDonald, and A. N. Syverud, JANAF Thermochemical Tables, Third Edition, J. Phys. Chem. Ref. Data, Suppl. 1 **14** (1985).
[58]R. L. Sams and W. J. Lafferty, J. Mol. Spectrosc. **125**, 99 (1987) and references therein.
[59]B. P. Winnewisser, in *Molecular Spectroscopy: Modern Research, Vol. III*, edited by K.N. Rao (Academic, Orlando, 1985), p. 321.
[60]M. Quack and J. Troe, Ber. Bunsenges, Phys. Chem. **81**, 329 (1977).
[61]G. D. Gillespie, A. U. Khan, A. C. Wahl, R. P. Hosteny, and M. Krauss, J. Chem. Phys. **63**, 3425 (1975).
[62]V. M. Donnelly and F. Kaufman, J. Chem. Phys. **66**, 4100 (1977); **69**, 1456 (1978).
[63]S. E. Stein and B. S. Rabinovitch, J. Chem. Phys. **58**, 2438 (1973).

[64]For an example, see J. R. Barker, Chem. Phys. **77**, 301 (1983).
[65]For a Master Equation treatment including angular momentum, see S. C. Smith and R. G. Gilbert, Int. J. Chem. Kinet. **20**, 307 (1988).
[66]G. Herzberg, *Infrared and Raman Spectra of Polyatomic Molecules* (Van Nostrand, Princeton, 1945), 501ff.
[67]J. V. Michael and J. H. Lee, J. Phys. Chem. **83**, 10 (1979).
[68]For example, see R. A. Marcus, Chem. Phys. Lett. **144**, 208 (1988).
[69]For example, see M. Lewerenz and M. Quack, J. Chem. Phys. **88**, 5408 (1988) and references therein.
[70]For example, see M. Quack, Ber. Bunsenges, Phys. Chem. **88**, 94 (1984).